Single-Molecule Imaging and Functional Analysis of Als Adhesins and Mannans during *Candida albicans* Morphogenesis

Audrey Beaussart,[†] David Alsteens,[†] Sofiane El-Kirat-Chatel,[†] Peter N. Lipke,[‡,*] Sona Kucharíková,[§,⊥] Patrick Van Dijck,[§,⊥,*] and Yves F. Dufrêne[†,*]

[†]Institute of Life Sciences & Institute of Condensed Matter and Nanosciences, Université catholique de Louvain, Croix du Sud, 1, bte L7.04.01., B-1348 Louvain-la-Neuve, Belgium, [‡]Department of Biology, Brooklyn College of City University of New York, Brooklyn, New York 11210, United States, and [§]Department of Molecular Microbiology, VIB and [⊥]Laboratory of Molecular Cell Biology, Institute of Botany and Microbiology, K.U. Leuven, 3000 Leuven, Belgium

ABSTRACT

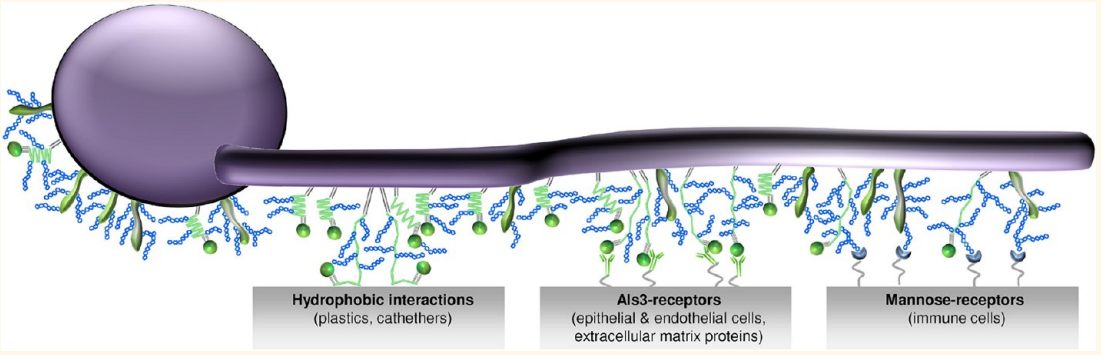

Cellular morphogenesis in the fungal pathogen *Candida albicans* is associated with changes in cell wall composition that play important roles in biofilm formation and immune responses. Yet, how fungal morphogenesis modulates the biophysical properties and interactions of the cell surface molecules is poorly understood, mainly owing to the paucity of high-resolution imaging techniques. Here, we use single-molecule atomic force microscopy to localize and analyze the key components of the surface of living *C. albicans* cells during morphogenesis. We show that the yeast-to-hypha transition leads to a major increase in the distribution, adhesion, unfolding, and extension of Als adhesins and their associated mannans on the cell surface. We also find that morphogenesis dramatically increases cell surface hydrophobicity. These molecular changes are critical for microbe–host interactions, including adhesion, colonization, and biofilm formation. The single-molecule experiments presented here offer promising prospects for understanding how microbial pathogens use cell surface molecules to modulate biofilm and immune interactions.

KEYWORDS: AFM · cellular morphogenesis · pathogens · molecular mapping · single-molecule manipulation

Many microbial infections involve adhesion of the pathogen to tissues and implanted devices and the subsequent formation of biofilms on these surfaces.[1−4] Because biofilms protect the pathogen from host defenses and are resistant to many antimicrobial agents, biofilm-related infections are difficult to fight. Therefore, understanding the molecular mechanisms underlying microbial adhesion and biofilm formation is a crucial challenge in current microbiology and a key in medicine for discovering the bases of infection processes and for developing new antimicrobial strategies.

Candida albicans, the most common fungal pathogen of humans, shows a remarkable ability to adhere to abiotic surfaces, cells, and tissues.[5,6] Many *C. albicans* infections result from the formation of biofilms on tissues, prosthetics, and catheters.[2,3] During invasion of host tissues and the bloodstream, *C. albicans* is recognized by the immune system which elicits an immune

* Address correspondence to yves.dufrene@uclouvain.be, Patrick.VanDijck@mmbio.vib-kuleuven.be, PLipke@brooklyn.cuny.edu.

Received for review September 28, 2012 and accepted November 1, 2012.

Published online November 12, 2012
10.1021/nn304505s

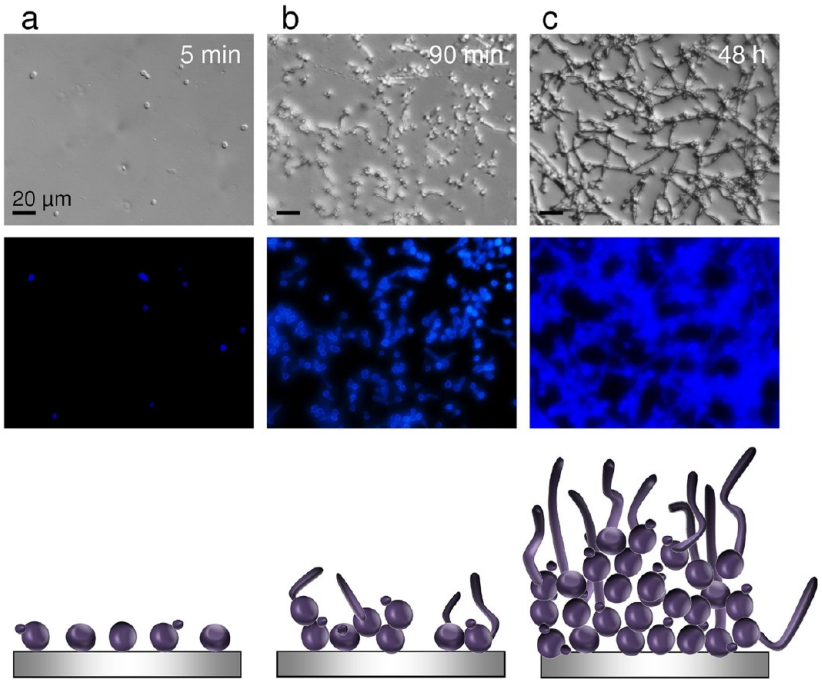

Figure 1. *Candida albicans* morphogenesis, cell adhesion, and biofilm formation. Phase contrast (top) and fluorescence (bottom) images of Calcofluor White stained *C. albicans* cells adhering on plastic surfaces after 5 min (a), 90 min (b), and 48 h (c). The cartoons underneath the images emphasize the different steps leading to biofilm formation and the role of yeast and hyphal cells in the process. Cells were grown overnight in YPD medium, inoculated in RPMI to induce germination, incubated at 37 °C with the plastic coverslips, and then rinsed with buffer solution.

response. Consequently, biofilm and immune interactions are determined by the major molecular components of the fungal cell surface, such as cell wall mannoproteins and polysaccharides, chiefly β-glucans and chitin. Specifically, cell surface mannoproteins called "adhesins"[5] mediate biofilm formation and are major antigens that can modulate immune responses.[7] On the other hand, mannose-rich structures on the *C. albicans* surface are recognized by a vast array of lectin receptors from the immune system, including dectins, macrophage mannose receptor, dendritic cell-specific ICAM3-binding non-integrin, macrophage-inducible C-type lectin, and the circulating mannose-binding lectin.[7] Understanding the role of adhesins and mannans in biofilm and immune interactions requires studying the localization, properties, and function of these molecules at the molecular level.

Fungal polymorphism is a remarkable trait of fungal pathogens in which the cells grow and form biofilms as either unicellular budding yeast cells or filamentous hyphae, that is, tubular projections that are compartmentalized into cellular units with nuclei. In *C. albicans*, both yeast cells and hyphae are crucial for biofilm formation, suggesting that each cell type has a unique role in the process.[2] Cellular morphogenesis is associated with changes in cell wall composition, and there are clear indications that this cell surface remodeling influences biofilm formation and the immune response. However, to what extent proteins and carbohydrates are differently exposed on yeast and hyphal surfaces is still poorly understood, owing to the lack of high-resolution imaging techniques.

Atomic force microscopy (AFM) is emerging as one of the most powerful imaging tools of the modern cell surface biologist, as is evident from the continuous increase in numbers of papers published in the field (for recent reviews, see refs 8 and 9). Originally invented for structural imaging, AFM has evolved into a multifunctional imaging tool, enabling researchers not only to observe structural details of cells but also to measure the localization, elasticity, and interactions of the individual molecules.[10,11] Continuous progress in sample preparation, data recording, and interpretation has enabled researchers to unravel the surface properties of cells from a wealth of organisms, from bacteria to humans. In the fungal context, AFM has been widely used to probe single proteins and polysaccharides on yeasts.[12−17] However, the imaging and manipulation of single molecules on growing fungal hyphae has long been hampered by technical difficulties. Here, we show that single-molecule AFM is a powerful tool for imaging and analyzing the functional components of the surface of *C. albicans* yeasts and hyphae, in relation to function. We find that the molecular properties (*i.e.*, distribution, adhesion, elasticity, and extension) of individual adhesins and their associated mannans on the two forms are very different, demonstrating that the yeast-to-hypha transition is associated with dramatic changes in the cell surface. This molecular remodeling strongly enhances cell surface hydrophobicity and

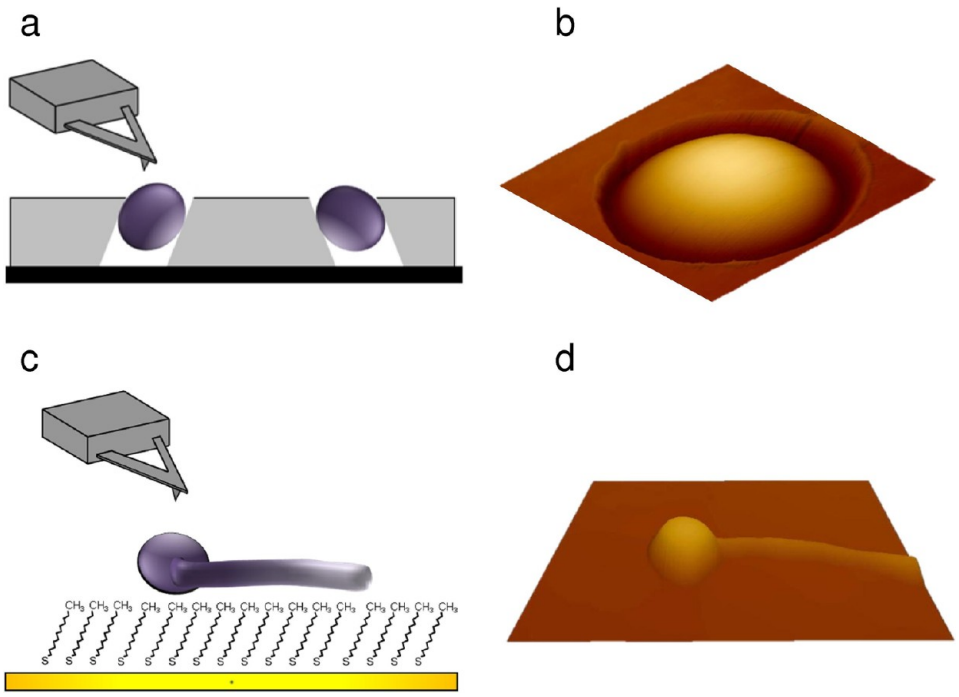

Figure 2. AFM imaging of living yeast cells and hyphae. Two different approaches were used to immobilize *C. albicans* yeast cells and hyphae nondestructively: (a,b) spherical yeast cells were immobilized mechanically into porous polymer membranes, while (c,d) germinating cells were attached onto solid substrata functionalized with hydrophobic groups. (b,d) Three-dimensional AFM images of a yeast-form cell (b; 5 μm × 5 μm) and of a germinating cell (d; 15 μm × 15 μm). The two methods are simple and do not involve drying or chemical treatments that could lead to denaturation of the cell surface molecules.

promotes fungal adhesion. The high-resolution method presented here is the only technique currently available to simultaneously image and manipulate the individual components of fungal cell walls, thereby contributing to increase our understanding of the biofilm and immune interactions of fungal pathogens.

RESULTS AND DISCUSSION

***Candida albicans* Dimorphism and Biofilm Formation.** To investigate the ability of *C. albicans* to attach to abiotic surfaces and to form biofilms, yeast-form cells were inoculated on polyethylene plates for 5 min, 90 min, and 48 h in conditions inducing germination (RPMI medium, 37 °C). Following adhesion, non-attached cells were removed by successive washing and the adhering cells were then stained with Calcofluor White.[18] As reported earlier,[18] biofilm formation started with the adhesion of yeast cells to the surface, followed by the formation of germ tubes and microcolonies (Figure 1). In a later stage, the biofilm biomass expanded and extracellular polymers accumulated.[3] While formation of hypha is important for biofilm formation, and in the subsequent colonization of the host,[7] little is known about the influence of morphogenesis on the exposure and biophysical properties of specific molecules on the cell surface.

Live-Cell Imaging. To address this issue, we developed protocols for imaging yeast and hyphal cells of *C. albicans* by AFM. Live-cell imaging requires attaching the cells firmly onto an appropriate substrate. As shown in Figure 2a,b, firm attachment of yeast cells was achieved by trapping the cells mechanically into a porous polymer membrane. As germinating hyphal cells could not be immobilized using this strategy, we tested several other approaches and we found that, unlike yeast cells, hyphae were strongly attached by letting them to adhere to hydrophobic alkanethiol monolayers (Figure 2c,d). This protocol, consistent with the hydrophobic properties of hyphal cells[19] (see also below), enabled us to image hyphae in liquid, without using chemical fixation or charged macromolecules, which is an important prerequisite for reliable single-molecular imaging.

Detection and Localization of Single Als3 Proteins on Yeast Cells. Adhesion of *C. albicans* is mediated by the Als family of cell surface glycoproteins.[5,20] Most *ALS* genes are differentially expressed in different phases of growth of the fungus. A striking example is Als3,[21] which plays a pivotal role in biofilm formation[22,23] and in modulating immune responses[7] and is known to be expressed primarily in germ tubes and hyphae.[21,24] Its deletion strongly affects *in vitro* biofilm formation, but not under *in vivo* conditions, probably due to higher expression of the homologous gene *ALS1* under these conditions.[22] Consistent with these reports, fluorescence microscopy using anti-Als3 antibodies and FITC-conjugated secondary antibodies revealed that the surface of wild-type (WT) germ tubes grown for 90 min was highly immunolabeled (Figure 3a,d), while the surface of WT yeast cells was poorly labeled (Figure 3b,e).

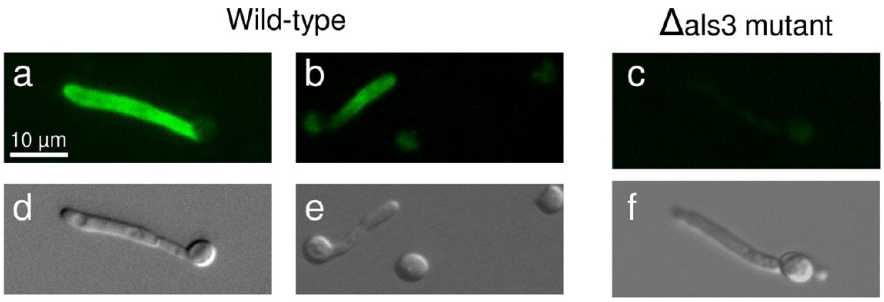

Figure 3. Fluorescence imaging of Als3 proteins. Fluorescence (a,b) and phase contrast (d,e) images of WT germinating (a,d) and yeast (b,e; see on the right) cells grown for 90 min in RPMI medium, stained with anti-Als3 antibodies followed by FITC-conjugated secondary antibodies. Unlike yeast cells, germ tubes were massively immunolabeled. Fluorescence (c) and phase contrast (f) images of a germ tube from an *als3*Δ/*als3*Δ (Δals3) mutant strain, revealing a lack of fluorescence. Similar results were obtained in independent experiments with cells from different cultures.

In addition, germ tubes from an *als3*Δ/*als3*Δ mutant strain deficient for Als3 expression did not show any fluorescence, confirming the specificity of the antibodies (Figure 3c,f). Note that, in these experiments, fungal cells were treated with goat serum to block nonspecific antibody binding.[24]

While fluorescence imaging localizes Als proteins in the cell wall, it lacks spatial resolution and does not provide information on the biophysical properties (adhesion, elasticity, extension) of the probed molecules. We therefore used AFM with tips functionalized with anti-Als3 antibodies to gain a molecular view of the Als3 cell surface properties (Figure 4a). To ensure single Als3 detection, the tip was functionalized with a PEG−benzaldehyde linker using a well-established protocol.[25] Figure 4b−d shows the adhesion force map, the adhesion force histogram with representative force curves, and the rupture length histogram recorded between the antibody tip and the surface of WT yeast cells. A moderate proportion (14%) of force curves showed adhesion signatures (Figure 4b,c) that we attribute to the detection of single Als proteins based on several control experiments (see below). Most proteins formed very small clusters, yielding a minimum protein surface density of ∼140 proteins/μm^2 (Figure 4b). Two different force signatures were observed, such as low adhesion force curves (Figure 4c, top curves) displaying single small adhesion forces (41 ± 15 pN) at fairly short distances (10−100 nm; Figure 4d), and high adhesion force curves (Figure 4c, bottom curves), showing sawtooth patterns with multiple large force peaks (331 ± 38 pN) and long ruptures (150−400 nm; Figure 4d). Assuming that yeast adhesins are 1100−2400 amino acids in length and that each amino acid contributes 0.36 nm to the contour length of a fully extended polypeptide chain, we found that our measured 150−400 nm rupture lengths correspond to the expected lengths of partially or fully extended proteins.

Previously, we demonstrated that the low/short and high/long force signatures reflect the dual detection of single Als by the anti-Als tip.[14,26] The low force peaks correspond to the weak molecular recognition of specific epitopes in the Als threonine-rich (T) and Ig-like regions. In contrast, the high force peaks represent the strong multipoint attachment of the Als Ig-like region to the antibody mounted on the tip, which acts as a ligand for the Als adhesin, in other words, reciprocal binding of Als to the probe antibody. This reciprocal Als binding to antibody leads to the sequential unfolding of the tandem repeat (TR) domains of Als upon pulling the tip.[14] To better visualize these dual detection events, three-dimensional (3-D) maps of polymer properties were constructed by combining adhesion forces and rupture distances measured on every position on the surface map (Figure 4e). The 3-D map obtained for the yeast cell surface documents the detection of both non-adhesive or weak events (gray) and strong (green) adhesion events, with short and long rupture lengths (*z*-axis). Our finding that, at the single-molecule level, Als proteins are detected on yeast-form cells suggests that Als3 may be more abundant on the surface of yeast cells than previously thought, and/or that other Als adhesins, like Als1, are probed by the antibody through cross-reactions. The apparent discrepancy between the moderate level of AFM detection and the poor fluorescence labeling may be explained by the major differences between the two techniques (see more details below). A key difference is that AFM was performed on native cells while fluorescence data were obtained after blocking the cell surface with serum.

Differential Surface Localization of Als3 Proteins on Hyphae. We then explored the spatial distribution of Als3 proteins on germinating cells, focusing both on the germinated yeast and on the germ tube regions (Figure 5). The Als3 distribution of the germinating yeast (Figure 5a−c) was different from that of the nongerminating yeast (Figure 4) in several respects: first, a higher detection frequency was observed, 33%, corresponding to a minimum protein surface density of ∼340 proteins/μm^2; second, most adhesion signatures were weak epitope binding events (32 *vs* 9% on nongerminating yeast) with rather short rupture lengths (10−200 nm), the

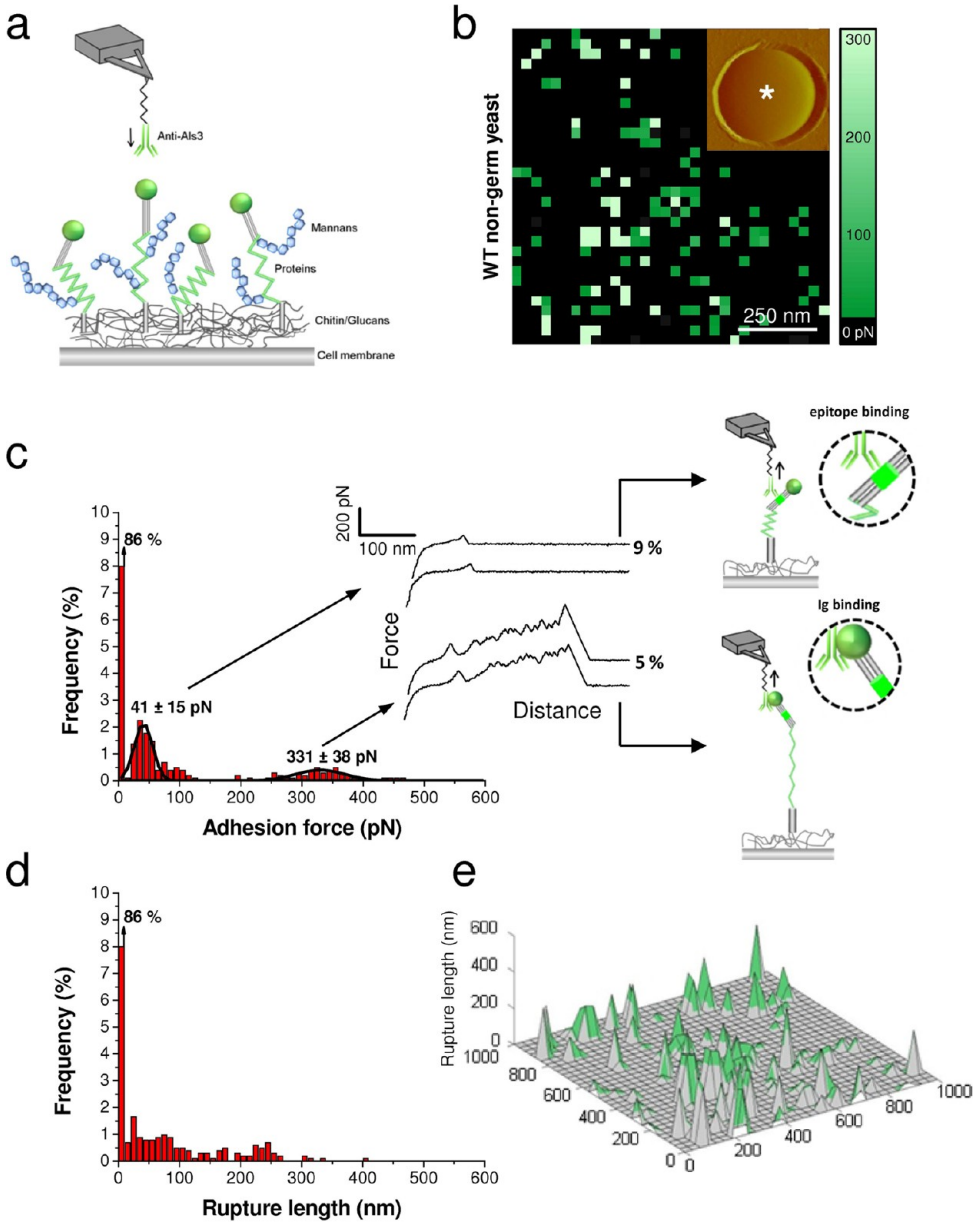

Figure 4. Single-molecule detection of Als3 proteins on yeast cells. (a) Cell wall in *C. albicans* is made of an inner layer of chitin and β1,3-glucan polysaccharides that confer strength and cell shape and an outer layer of mannose polymers, mannans (blue), covalently associated with cell wall proteins such as Als adhesins (green). To probe single Als3 proteins, *C. albicans* yeast cells were imaged in buffer using AFM tips terminated with an anti-Als3 antibody. (b–d) Adhesion force map (b; 1 μm × 1 μm, color scale: 300 pN), adhesion force histogram (n = 1024 force curves) together with representative force curves (c), and rupture length histogram (d) obtained by recording force curves across the surface of a *C. albicans* yeast-form cell using an antibody-labeled tip. The inset in (b) is a deflection image of the cell in which the * symbol indicates where the force map was recorded. The cartoons in (c) emphasize the dual detection of Als3: while some curves showed single weak adhesion peaks reflecting Als epitope recognition (top curves), others featured sawtooth patterns with multiple force peaks documenting Als Ig-to-ligand multipoint binding followed by the unfolding of the entire protein (bottom curves). (e) Three-dimensional reconstructed map obtained by combining adhesion force values (false colors, adhesion forces are shown in green) and rupture distances (expressed as z level) measured at different x, y locations. Unless stated otherwise, all curves were obtained at 20 °C using a contact time of 100 ms and a loading rate of 10 000 pN s^{-1}. Similar data were obtained in several independent experiments using different tip preparations and cell cultures.

frequency of strong unfolding events being negligible (1 *vs* 5%); and third, most Als3 proteins seemed to form clusters of 100–500 nm equivalent diameter, somewhat similar to the clusters previously observed for Als5 on force-activated *ALS5* expressing *Saccharomyces cerevisiae* cells.[14] However, unlike Als5 clustering, Als3 clustering did not seem to require preactivation by mechanical force. These observations suggest that the amount of Als3 exposed on the surface of the yeast region increases upon germination, and that they form large clusters without the help of an external force. A possible explanation for this behavior is that Als3 clustering observed during germination is induced by mechanical stress associated with adhesion to the

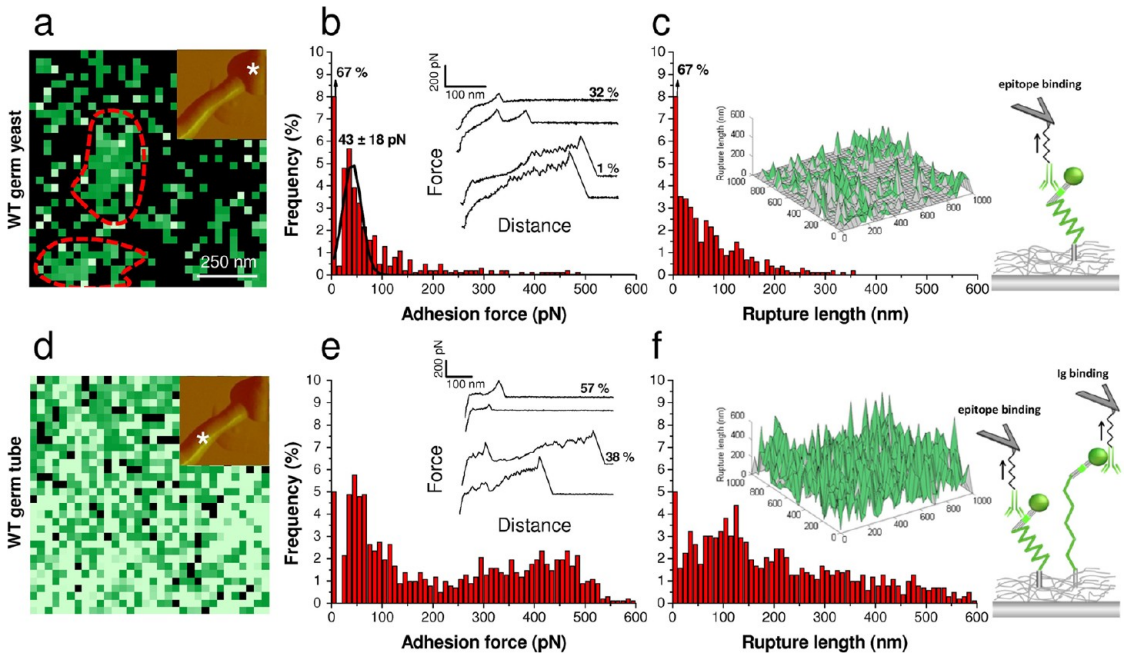

Figure 5. Cellular morphogenesis leads to a major increase in the distribution and extension of Als3 proteins. (a,d) Adhesion force maps (1 μm $\times$ 1 μm, color scale: 300 pN) recorded in buffer on the yeast (a) and germ tube (d) of a germinating cell using an anti-Als3 tip. Insets: deflection images in which the * symbols indicate where the force maps were recorded. The dashed lines in (a) emphasize Als3 clusters. (b,e) Corresponding adhesion force histograms (n = 1024) together with representative force curves. (c,f) Histograms of rupture distances (n = 1024) and 3-D reconstructed polymer maps (false colors, adhesion forces in green). Similar data were obtained in several independent experiments using different tip preparations and cell cultures.

hydrophobic substrate or due to cell wall remodeling itself. Such remodeling stress is reminiscent of the mechanism recently proposed for the clustering of the cell integrity sensor Wsc1 in living *S. cerevisiae* cells.[16] Single-molecule AFM showed that clustering of the sensor proteins was strongly enhanced under stressing conditions, a phenomenon attributed to conformational changes resulting from stress-induced deformation of the cell wall.

Importantly, we found that the distribution and biophysical properties of Als adhesins on the germ tube (Figure 5d–f) were very different from those on the germinating yeast (Figure 5a–c). Adhesion events were detected in almost all locations (95%), documenting the massive exposure of adhesins corresponding to a minimum protein surface density of ~970 proteins/μm^2. In addition, the number of unfolding events dramatically increased (38 *vs* 1% on germinating yeast cells), together with an increase of the rupture lengths. The measured unfolding lengths were up to 600 nm, thus larger than those on nongerminating yeasts (150–400 nm), a finding that may be due to the fact that some of the stretched proteins were indeed longer, and/or that cell wall glycans were stretched, as well. The 3-D map obtained for the germ tube clearly shows the massive detection and unfolding of single Als adhesins (Figure 5f, inset), which is in contrast with the yeast region which shows a much lower adhesin surface concentration with very infrequent unfolding (Figure 5c, inset).

Specificity of Als3 Detection. To determine the specificity of the measured binding events, four independent sets of control experiments were performed, that is, blocking with free antibodies, blocking with goat serum, use of mutant strains deficient for Als expression, and use of an AFM tip bearing an irrelevant antibody. Figure 6a–c presents the results of a blocking experiment with free antibodies, that is, the classical control in AFM molecular recognition studies. As can be seen, treating WT germ tubes with free anti-Als3 antibodies led to a major reduction of adhesion frequency (from 95 to 41%), indicating that a large fraction of the binding events indeed reflected Als3 adhesins.

In fluorescence studies, treatment of fungal cells with serum is a classical control to block nonspecific antibody binding (Figure 3). However, to the best of our knowledge, such treatment has never been used in AFM experiments. Interestingly, Figure 6d–f shows that blocking WT germ tubes with goat serum led to a dramatic reduction of detection frequency (from 95 to 22%) and, most importantly, to the disappearance of strong interactions with unfolding signatures (1% remaining). This indicates (i) that serum proteins masked most of the Ig-like regions of Als proteins, making them no longer accessible for Als-to-ligand reciprocal multipoint attachment and subsequent unfolding, and (ii) that the remaining fraction (21%) of weak force signatures indeed reflect specific Als epitopes recognized by the antibody. These data strongly support our dual detection model (Figure 4) and emphasize, for the first

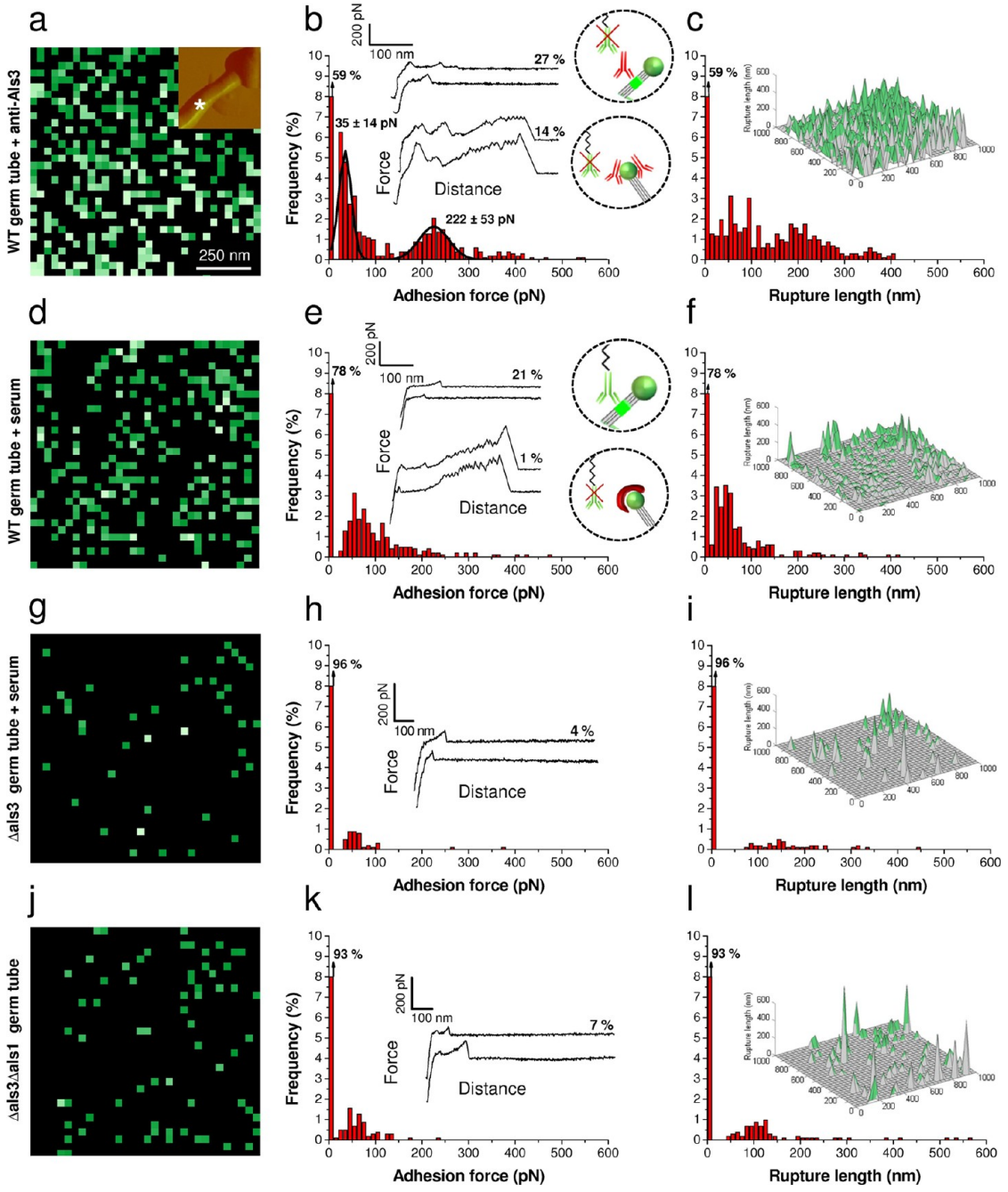

Figure 6. Control experiments demonstrate the specificity of Als3 detection. (a,d,g,j) Adhesion force maps (1 μm × 1 μm, color scale: 300 pN) recorded in buffer with anti-Als3 tips on WT germ tubes after treatment with free anti-Als3 antibodies (0.1 mg/mL) (a) or goat serum (d), on a *als3*Δ/*als3*Δ (Δals3) germ tube blocked with goat serum (g), and on a nonblocked *als3*Δ/*als3*Δ *als1*Δ/*als1*Δ (Δals3Δals1) germ tube (j). (b,e,h,k) Corresponding adhesion force histograms (*n* = 1024) together with representative force curves. (c,f,i,l) Histograms of rupture distances (*n* = 1024) and 3-D reconstructed polymer maps (false colors, adhesion forces in green).

time in an AFM study, the importance of control experiments with nonspecific serum in order to separate the relative contributions of specific epitope binding events and strong unfolding events.

To further demonstrate that the weak recognition events detected on native (57%, Figure 5d−f) and serum-blocked (21%, Figure 6d−f) germ tubes are due to Als3 epitopes, and not to other Als epitopes, we analyzed an *als3*Δ/*als3*Δ mutant strain. As shown in Figure 6g−i, *als3*Δ/*als3*Δ germ tubes blocked with serum displayed a very low detection frequency (4%), thus confirming that most recognition forces measured on WT germ tubes were indeed specific to Als3 epitopes. By contrast, *als3*Δ/*als3*Δ germ tubes that were not blocked with serum (Supporting Information Figure 1) showed a high detection frequency (85%) with numerous unfolding events (29%), indicating that other Als proteins, presumably Als1, were detected.

Indeed, the transcription factor Bcr1 mediates Als1 overexpression in order to compensate the Als3 defect in *als3*Δ/*als3*Δ mutants.[22] Supporting this view, we found that germ tubes from the double mutant *als3*Δ/*als3*Δ *als1*Δ/*als1*Δ showed only few adhesion events (7%), even in the absence of serum (Figure 6j–l).

Lastly, WT germ tubes were mapped with an irrelevant probe (*i.e.*, an AFM tip modified with an antibody directed against V5 epitopes; Supporting Information Figure 2). The use of irrelevant antibodies clearly leads to a major reduction of the low force Als3 epitope interactions (11 *vs* 57%), while the high force interactions remained. As expected, these strong interactions were inhibited following pretreatment of the germ tubes with nonspecific serum. The above findings lead us to conclude (i) that both Als3 and Als1 proteins contribute to the force signatures massively detected on WT germ tubes, without substantial contribution of other cell surface constituents, and (ii) that the contribution of Als3 can be isolated by treating the cells with serum or by using cell wall mutants.

A pertinent question is whether our single-molecule AFM data are consistent with fluorescence results. AFM of native germ tubes revealed they were almost fully covered with Als proteins (95%), in agreement with a high level of fluorescence labeling. After serum blocking, however, the AFM detection frequency was lower (22%, Figure 6e) because the AFM tip could no longer bind the epitopes on Als proteins, while fluorescence signal was high. This observation may be explained by the major differences between the two techniques. First, fluorescence labeling usually involves prolonged contact, and it is well-known that the binding probability in AFM studies strongly depends on the contact time between a receptor and its cognate ligand. Consistent with this, we found that the detection frequency between serum-blocked germ tubes and the anti-Als3 tip increased from 29 to 69% when increasing the contact time from 100 ms to 2 s (Supporting Information Figure 3). Note that molecular force mapping of fungal cells at prolonged contact times is extremely difficult with current technology (drift, tip alteration, cell damage, *etc.*). Second, the probabilities of antibody binding in AFM and fluorescence are likely to be very different due to differences in antibody concentration. In AFM, a single antibody fishes a single cell surface molecule for a very short period of time, then moves to another location, while in fluorescence, the whole cell surface is saturated with a solution of antibodies for prolonged contact time. Despite these differences, AFM and fluorescence data are in qualitative agreement.

Taken together, the above observations provide the first single-molecule evidence for the differential surface localization and biophysical properties of Als3 on germinating cells of *C. albicans*. The adhesin is much more exposed on the germ tube than on the germinating yeast cell, consistent with the notion that the *ALS3* gene is among the most highly upregulated genes during the yeast-to-hypha transition.[21] In addition, our results suggest major differences in protein conformational properties and mechanical stability, mechanical unfolding of the adhesins being only observed on the germ tube. Hence, AFM is a powerful complement to fluorescence in that it enables observation of live cells at nanometer resolution and under physiological conditions, to localize cell surface constituents at the level of single molecules, and to quantify the biophysical properties of individual molecules, including their adhesion, unfolding, and extension, in relation to cellular function (cell adhesion).

Als3 Expression Correlates with Cell Surface Hydrophobicity. Cell surface hydrophobicity is believed to be an important driving force for *C. albicans* adhesion.[27–29] Als proteins are thought to contribute to surface hydrophobicity *via* their hydrophobic TR domains that mediate adherence to hydrophobic substrates and can be unravelled by mechanical force.[26,30] We therefore postulated that the enhanced exposure of Als3 on hyphae may contribute to increase their hydrophobicity and, in turn, fungal adhesion to hydrophobic substrata. To test this hypothesis, we mapped and quantified the hydrophobicity of *C. albicans* cells with nanoscale resolution using AFM tips functionalized with hydrophobic groups (CH_3), a method known as chemical force microscopy (CFM)[31] (Figure 7). Force curves recorded on WT yeast cells (Figure 7a–c) showed only few, evenly distributed adhesion forces (8%) with moderate magnitude (50–1000 pN) and short rupture lengths (10–50 nm). By contrast, all curves (100%) obtained on WT germ tubes (Figure 7d–f) showed large adhesion forces (500–4000 pN) with extended rupture lengths (50–700 nm).

In the light of data obtained on reference surfaces,[31] we conclude that the yeast surface is hydrophilic, while the germ tube surface has very strong hydrophobic properties, somewhat similar to those measured for *Aspergillus fumigatus* hydrophobins.[31] A unique feature of the *C. albicans* germ tube, though, is the extended rupture lengths of the force signatures, together with multiple poorly defined peaks, suggesting that hydrophobicity may be associated with protein unfolding. As the average forces (500–4000 pN) are much larger than those associated with single protein binding and unfolding, it is therefore likely that these signatures result from multiple Als unfolding interactions. Such a behavior is fully consistent with differences in tip chemistry: while single-molecule imaging with antibody tips (Figure 4) relies on the use of a well-established protocol that ensures single-molecule detection,[25] CFM uses tips that are coated with a dense monolayer of hydrophobic groups (CH_3). As a result, ~40 CH_3 groups interact with the cell surface and are thus likely to simultaneously bind multiple proteins.

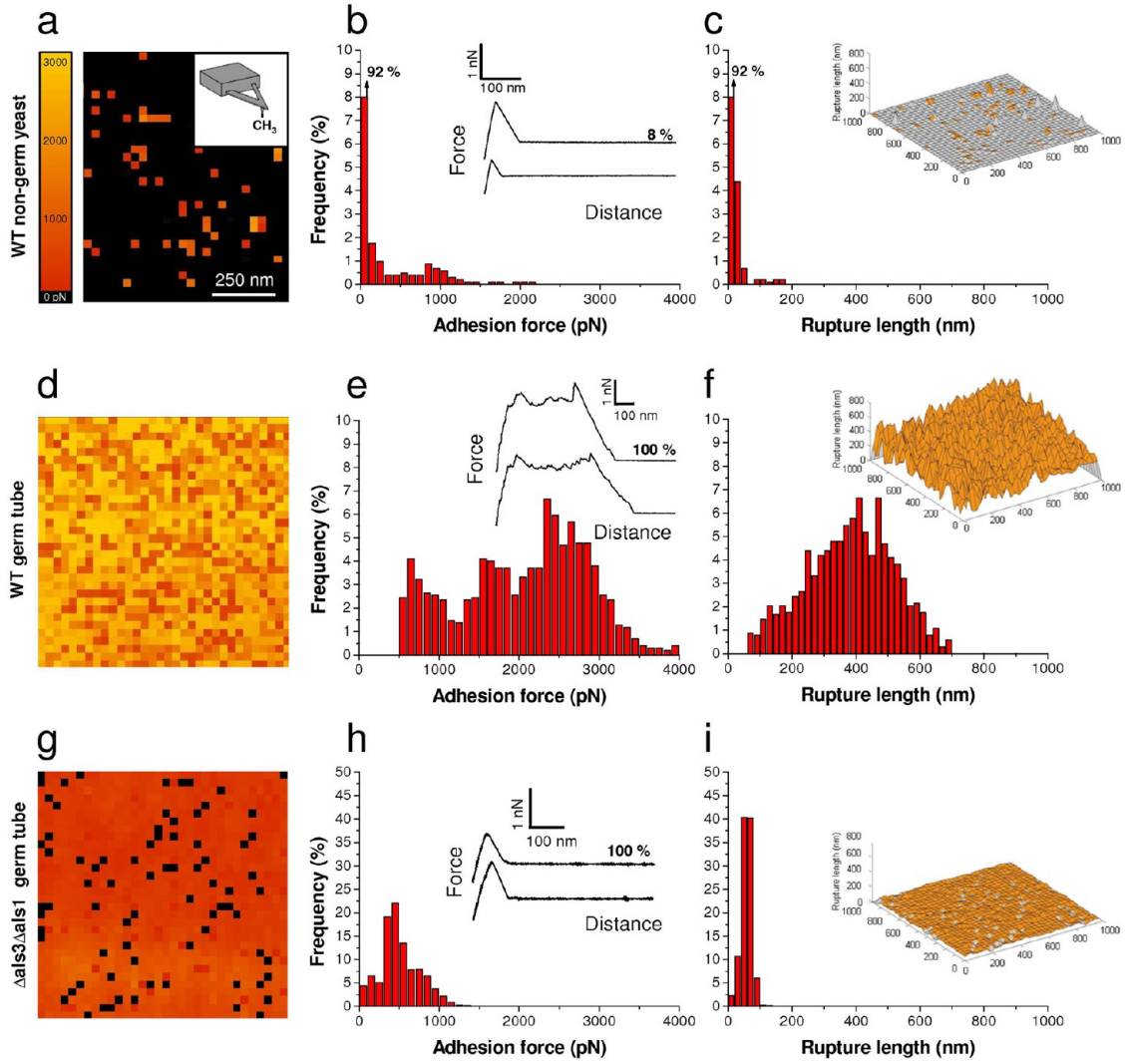

Figure 7. Cell surface hydrophobicity dramatically increases during cellular morphogenesis. (a,d,g) Adhesion force maps (1 μm $\times$ 1 μm, color scale: 3000 pN) recorded in buffer on a nongerminating WT yeast cell (a), a WT germ tube (d), and an *als3*Δ/*als3*Δ *als1*Δ/*als1*Δ (Δals3Δals1) germ tube (g) using hydrophobic tips. (b,e,h) Corresponding adhesion force histograms (*n* = 1024) together with representative force curves. (c,f,i) Histograms of rupture distances (*n* = 1024) and 3-D reconstructed hydrophobicity maps (false colors, adhesion forces in orange). Similar data were obtained in independent experiments using different tips and cultures.

To demonstrate that the strong hydrophobic properties of WT germ tubes are associated with Als3 proteins, CFM was applied to the double mutant *als3*Δ/*als3*Δ *als1*Δ/*als1*Δ. As shown in Figure 7g−i, all of the curves featured adhesion forces that were much smaller than those on the WT germ tube, and importantly, extended rupture lengths were missing. This finding, together with our Als3 data (Figure 5), provides direct evidence that cell surface hydrophobicity in *C. albicans* germ tubes originates from Als3 (and Als1) proteins, presumably through the exposure of their hydrophobic TR domains. Our results also show that CFM is a valuable method for imaging and quantifying the nanoscale surface hydrophobicity of fungal cells, including mutants, in a way that was not possible before.

Germination-Dependent Surface Properties of Mannan Glycoconjugates. While the genes encoding Als3 proteins are highly upregulated during the yeast-to-hypha switch, it is unclear whether the structure of the various mannans decorating the cell surface also differs between the yeast cells and hyphae. To tackle this problem, we used single-molecule AFM imaging with tips labeled with the lectin Concanavalin A (ConA) to probe the distribution and extension of mannan glycoconjugates on the two fungal forms. Figure 8a−c shows the adhesion force map, the adhesion histogram with representative force curves, and the rupture length histogram recorded on the surface of yeast cells with a ConA tip. The curves showed essentially single (or double) weak recognition events of 67 $\pm$ 30 pN magnitude, with rupture lengths ranging from 10 to 200 nm, that were distributed across the cell surface. In the light of previous work[15] and of blocking experiments (see below), these recognition signatures can be

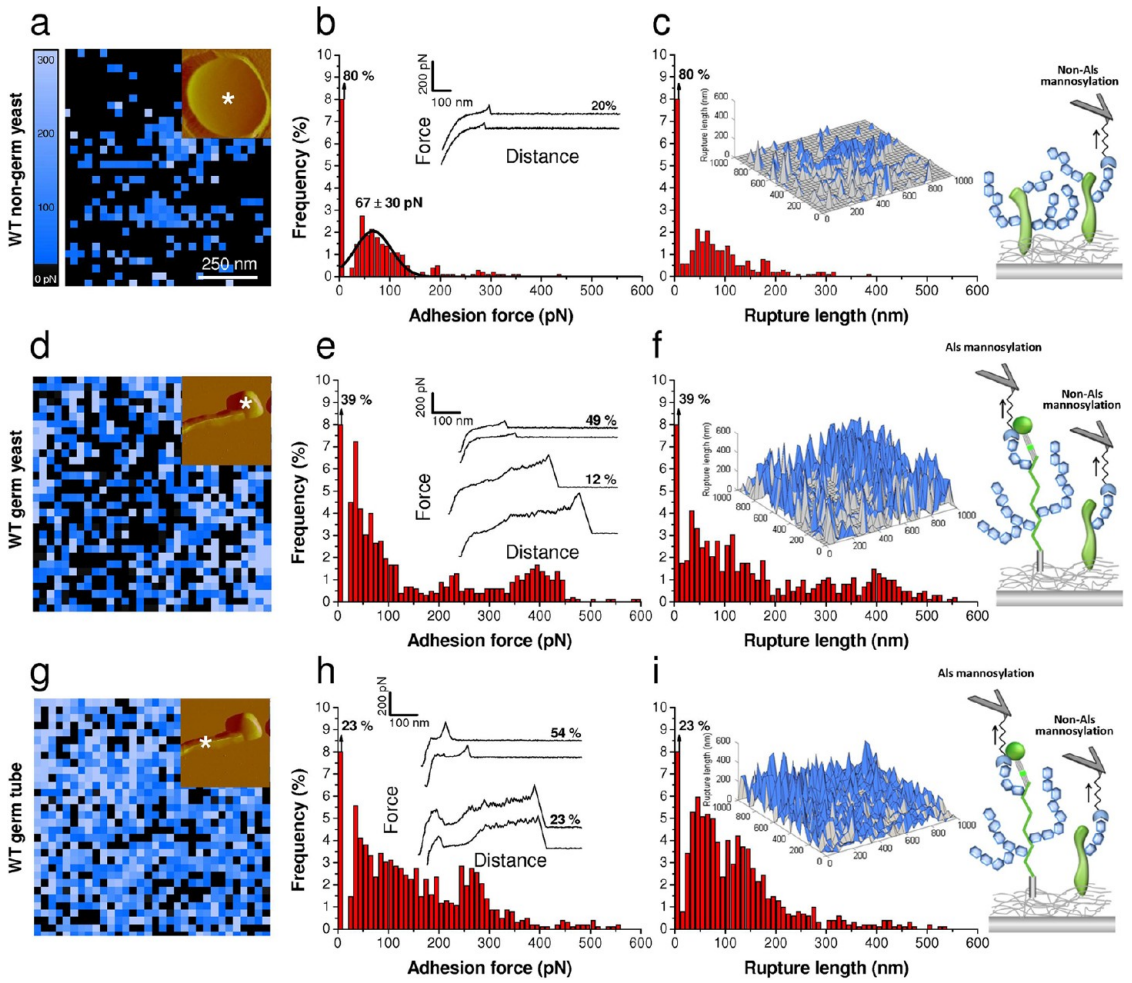

Figure 8. Imaging and stretching single mannan glycoconjugates during cellular morphogenesis. (a,d,g) Adhesion force maps (1 μm $\times$ 1 μm, color scale: 300 pN) recorded in buffer on a nongerminating yeast (a), on a germinating yeast (d), and on a germ tube (g) using an AFM tip labeled with ConA lectins. Insets: deflection images in which the * symbol indicates where the force maps were recorded. (b,e,h) Corresponding adhesion force histograms together with representative force curves. (c,f,i) Histograms of rupture distances (n = 1024) and 3-D reconstructed polymer maps (false colors, adhesion forces in blue). Similar data were obtained in independent experiments using different tips and cultures.

attributed to the detection of single mannose residues associated with mannoproteins. The distribution and extension of the mannan chains observed on *C. albicans* are quite similar to those measured earlier on *S. cerevisiae* brewing yeast strains.[15] We note that our measured rupture lengths are in the range of the outer-wall mannan fibril length measured recently by transmission electron microscopy (TEM; ~116 nm).[32] Yet, it is not surprising that some of our rupture distances are longer than the fringe thickness, as (i) electron microscopy is performed in the dried state and (ii) AFM distances represent the lengths of mechanically stretched glycopolymers.

Single-molecule imaging revealed major changes in mannan properties during cellular morphogenesis. Figure 8d–f shows that the surface density (61%) and extension (10–500 nm) of the mannose-rich glycoconjugates were higher on germinating yeast cells than on nongerminating ones, a difference that can be further visualized in the 3-D maps (see insets in Figure 8f *vs* 8c). Interestingly, a substantial fraction (12%) of the force signatures showed strong interactions (>200 pN) with sawtooth patterns with large rupture lengths, reflecting mannoprotein unfolding. These signatures are consistent with strong reciprocal binding of Als proteins, with ConA acting as the ligand, thus similar to Als binding to the antibody probe. As we shall demonstrate below, these mechanical signatures indeed represent the detection and subsequent unfolding of Als proteins, facilitated by initial weak binding of the lectin to Als mannosyl residues.[7,20,33] These force-induced protein unfolding events also explain our very long rupture lengths (up to 500 nm), much longer than the ~116 nm mannan fibril length measured by TEM.[32]

Imaging of germ tubes demonstrated a more abundant distribution of mannosylations than on yeast cells (77%), with a higher proportion of both weak recognition events (54%) and strong unfolding events (23%) (Figure 8g–i; Supporting Information Figure 4). Notably, analysis of the quintuply mutated strain

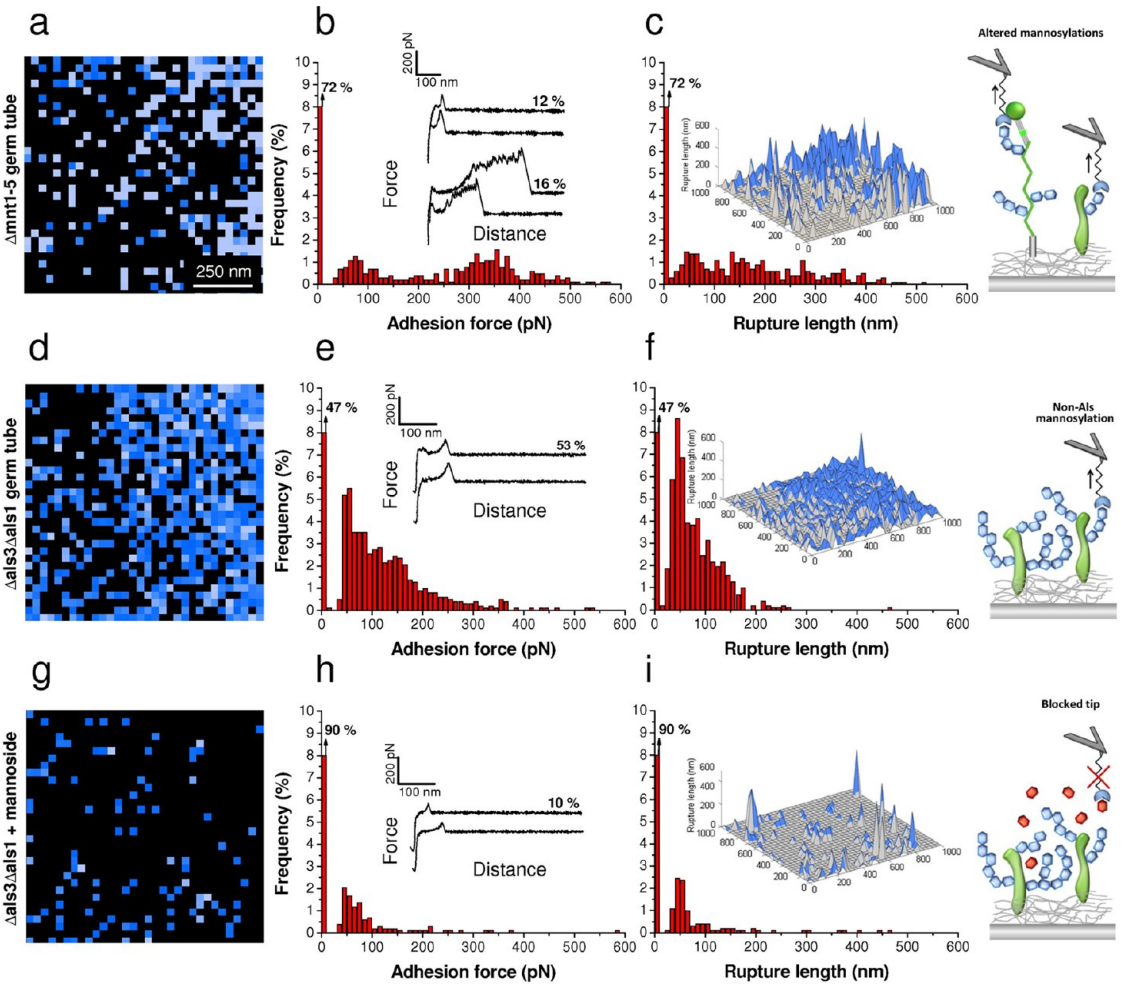

Figure 9. Probing mannans on cell wall mutants. (a,d,g) Adhesion force maps (1 μm × 1 μm, color scale: 300 pN) recorded in buffer with a Con A tip on a *mnt1*Δ/*mnt1*Δ *mnt2*Δ/*mnt2*Δ *mnt3*Δ/*mnt3*Δ *mnt4*Δ/*mnt4*Δ *mnt5*Δ/*mnt5*Δ (Δmnt1−5) germ tube altered in O-linked and N-linked mannosylations (a), on a *als3*Δ/*als3*Δ *als1*Δ/*als1*Δ (Δals3Δals1) germ tube (d), and on a *als3*Δ/*als3*Δ *als1*Δ/*als1*Δ (Δals3Δals1) germ tube blocked with 200 mM methyl α-D-mannopyranoside (g). (b,e,h) Corresponding adhesion force histograms together with representative force curves. (c,f,i) Histograms of rupture distances (n = 1024) and 3-D reconstructed polymer maps (false colors, adhesion forces in blue). Similar data were obtained in independent experiments using different tips and cultures.

*mnt1*Δ/*mnt1*Δ *mnt2*Δ/*mnt2*Δ *mnt3*Δ/*mnt3*Δ *mnt4*Δ/*mnt4*Δ *mnt5*Δ/*mnt5*Δ defective in O-linked and N-linked mannosylations revealed a substantial reduction of mannosylations, both in terms of short/weak and long/strong events (Figure 9a−c). This shows that AFM is capable of detecting changes in the level and nature of protein mannosylations in cell wall mutants, and that it should therefore be a valuable tool in future phenotypic studies of *C. albicans* glycosylation mutants.

Next, we addressed the origin of the weak and strong binding events by analyzing the double mutant *als3*Δ/*als3*Δ *als1*Δ/*als1*Δ. Figure 9d−f reveals that double mutant germ tubes showed the same amount of weak recognition events as the WT but a complete lack of unfolding signatures. The same behavior was observed by blocking WT germ tubes with nonspecific serum (Supporting Information Figure 5d−f). These independent experiments demonstrate that weak recognition events are associated with mannosylations while strong unfolding events reflect Als binding. Our measured lengths for mannosylations, 10 to 200 nm, are similar to those measured on yeast cells and roughly in the range of the ∼73 nm mannan fibril length measured by TEM.[32] We further assessed the specificity of the weak recognition events by blocking *als3*Δ/*als3*Δ *als1*Δ/*als1*Δ germ tubes with free α-methyl mannoside. Figure 9g−i shows that treatment of the double mutant with mannoside led to a much lower frequency of adhesion events (from 53 to 10%), indicating that they are associated with non-Als mannosylations. The same result was observed by treating serum-blocked WT germ tubes with mannoside (Supporting Information Figure 5g−i). Thus, the weak interactions showed the characteristics of ConA binding to α-mannosyl groups, while the strong events again had the properties of Als Ig regions binding to a ligand.

To summarize, our data show that, although the general composition of the cell walls of the different

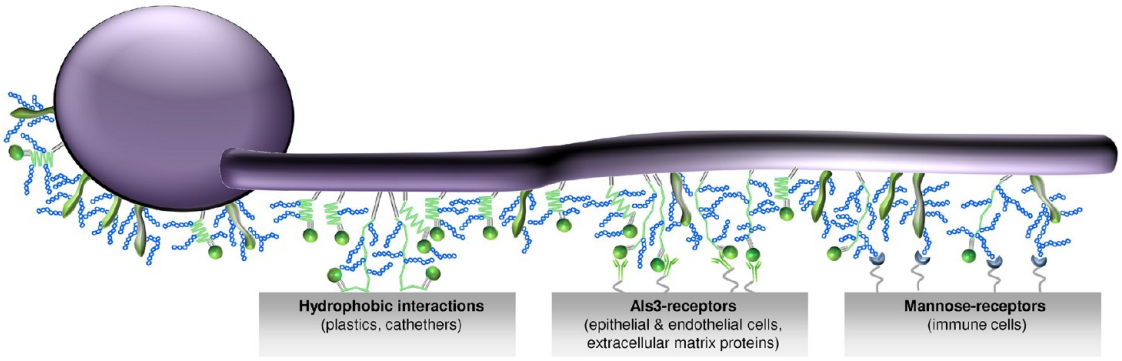

Figure 10. Toward a molecular and functional view of Als3 and mannans during *Candida albicans* morphogenesis. Germination of *C. albicans* leads to a major increase in the distribution and extension of Als3 proteins (green) and their associated mannans (blue) on the hyphae surface, a phenomenon which promotes adhesion to various surfaces (see text for details).

C. albicans forms (nongerminating yeasts, germinating yeasts, and hyphae) are similar,[7] the distribution and properties of the various macromolecules show major differences. Our main finding is that Als3 adhesins and mannans are not only more abundant on hyphae but that they are also more sticky and more extended, providing evidence that these components are important for cell surface interaction (biofilm formation, immune response). The results also emphasize major differences between nongerminating and germinating yeasts, a behavior which until now had been overlooked.

CONCLUSIONS

Understanding how *C. albicans* morphogenesis modulates the molecular composition and interactions of the fungal cell surface is an important, yet still unsolved, issue in microbiology. Our single-molecule experiments demonstrate that germination of *C. albicans* leads to a major increase in the distribution, adhesion, unfolding, and extension of Als3 adhesins and mannosylations on the cell surface. These changes are accompanied by a major increase in cell surface hydrophobicity. We believe these cell surface changes are function-related as they may play key roles in promoting adhesion to biotic and abiotic surfaces (Figure 10). Applicable to a wide variety of fungal species, these single-molecule analyses open new avenues for tracking the molecular components of hyphae in the context of cellular morphogenesis and for understanding their involvement in pathogenesis and host defense.

Our finding that the surface density, adhesiveness, and unfolding of Als proteins strongly increase on hyphae is fully consistent with the notion that the *ALS3* gene is highly expressed and upregulated during the morphogenetic switch[21] and provides new insights into the molecular mechanisms underlying fungal adhesion and biofilm formation. In addition, we have also shown that Als1 proteins are also highly expressed during morphogenesis, at least on cells deleted for Als3. We propose a model in which the adhesion of germinating cells is activated by the combination of two factors, that is, the expression of Als3 (and Als1) in large amounts and the mechanically induced exposure of hydrophobic sequences (Figure 10). We expect that the large amounts of Als TR domains on germ tubes and their force-induced unfolding will lead to extended conformations in which hydrophobic groups are freshly exposed and favor hydrophobic interactions. Supporting this view, pioneering studies have shown that cell surface hydrophobicity plays a role in the adhesion of *C. albicans* to biotic and abiotic surfaces.[27−29] Germ tubes are thought to largely contribute to hydrophobicity,[34] but the molecular origin of this enhanced hydrophobicity is unclear. Our data strongly suggest a model in which surface hydrophobicity originates both from the inherent hydrophobicity of Als TR domains and from their force-induced exposure and unfolding. In nature, mechanical contacts between the cells and other surfaces will generate forces that are strong enough to unravel Als proteins, thereby strengthening adhesion (Figure 10, left). In addition to enhancing hydrophobic interactions, Als unfolding may also change the exposure and conformation of the N-terminal Ig domains and, in turn, promote specific adhesion to host constituents (Figure 10, center), including epithelial cells, endothelial cells, and extracellular matrix proteins, and the subsequent colonization of mucosal surfaces. As a matter of fact, Als3 proteins have been shown to bind to N-cadherin on endothelial cells and E-cadherin on oral epithelial cells through their N-terminal portion.[35] This interaction is similar to cadherin−cadherin binding, providing evidence that Als3 is a molecular mimic of human cadherins. Our proposed mechanism is reminiscent of the cryptic sequences found in animal cell proteins involved in cell adhesion and mechanosensing (*e.g.*, spectrin, talin, titin, fibronectin, and cadherins), known to contain sequences that can be unraveled by force and lead to alterations in molecular recognition sites or the exposure of new peptide sequences.[36]

Our experiments also show that formation of hyphae is accompanied by an increase in the exposure and extension of mannosylations. Expression of Als proteins contributes to these mannosylations because these proteins are highly expressed in the germ tubes and heavily glycosylated. This finding is likely to be important for the interaction with epithelium cells and with the immune system. Differential localization and structure of mannose-rich molecules on hyphae *versus* yeast cells have been suggested to play a role in epithelial cell adhesion, endocytosis, colonization, penetration, and invasion.[7] Furthermore, as these glycoconjugates are recognized by a wide range of receptors from the immune system, differences in mannan properties may also modulate the immune response (Figure 10, right). For instance, differential dectin-mediated recognition of mannans from hyphae and yeast cells has been suggested, but the differences in mannan structure that are responsible for these effects are still unclear.[7]

METHODS

Microorganisms and Cultures. *C. albicans* SC5314[37] was cultivated on YPD medium (1% yeast extract, 2% Bacto-peptone, 2% D-glucose, supplemented with 2% agar) at 30 °C. A few colonies were inoculated in YPD liquid medium and incubated overnight (30 °C, 200 rpm). Yeast cells were harvested by centrifugation, washed three times with sodium acetate buffer, and resuspended in 10 mL of buffer to a concentration of $\sim 1 \times 10^6$ cells/mL. For hyphae formation, germination was induced by inoculating 250 μL of cell suspension in 8 mL of RPMI 1640 medium buffered with MOPS (Sigma) at pH 7 and incubated at 37 °C, 200 rpm, for 90 min unless otherwise stated.[18]

We used mutant strains with deletion of both alleles of *ALS* genes (kindly provided by Aaron Mitchell, Carnegie Mellon University, Pittsburgh, PA).[23] These mutants were derived from CAI-4[38] and included the simple mutants *als1*Δ/*als1*Δ (Δals1)[30] and *als3*Δ/*als3*Δ (Δals3)[22] and the double mutant *als3*Δ/*als3*Δ *als1*Δ/*als1*Δ (Δals3Δals1).[23] We also used the mutant strain *mnt1*Δ/*mnt1*Δ *mnt2*Δ/*mnt2*Δ *mnt3*Δ/*mnt3*Δ *mnt4*Δ/*mnt4*Δ *mnt5*Δ/*mnt5*Δ (Δmnt1−5) in which both alleles of *MNT1−5* genes were deleted, yielding defective O-linked and N-linked mannosylations (kindly provided by Neil Gow, University of Aberdeen, UK).[39]

Biofilm Assays. Cell adhesion and biofilm formation were assayed on highly adhesive, round tissue culture coverslips (diameter 13 mm, Sarstedt) using optical and fluorescence imaging. Five hundred microliters of a cell suspension (1×10^6 cells/mL) prepared in RPMI was added to a well of a clean 24-well tissue culture plate containing a coverslip and incubated at 37 °C. After 5 min, 90 min, or 48 h, the coverslips were gently rinsed with 2 × 1 mL of acetate and transferred to a clean well containing 300 μL of acetate with 5 μL of Calcofluor White (5 mg/mL). Images were acquired with a Zeiss Axio Observer Z1 equipped with a Hamamatsu camera C10600.

Fluorescence Microscopy. Following germination for 90 min in RPMI, cells were washed twice by centrifugation in buffer. Cells were resuspended in 15 μL/mL normal goat serum (Sigma) for 15 min at room temperature to block nonspecific antibody binding and washed twice in buffer. They were further incubated in a 18 μg/mL solution of anti-Als3 antibodies (kindly provided by Dr. Scott Filler, Harbor-UCLA Medical Center)[35] for 60 min at 4 °C and then in a 3 μg/mL fluorescein isothiocyanate (FITC)-conjugated goat anti-mouse IgG $F(ab')_2$ fragment-specific antibody (Jackson ImmunoResearch 115-096-006) for 60 min. Images were acquired with a Zeiss Axio Observer Z1 equipped with a Hamamatsu camera C10600.

Atomic Force Microscopy. AFM measurements were performed at room temperature (20 °C) in sodium acetate buffer supplemented with Ca^{2+} and Mn^{2+} at 1 mM (Con A tips) or not (Als3 imaging), using either a Nanoscope V Multimode AFM (yeast cells) or a Bioscope catalyst (hyphae) from Bruker Corporation (Santa Barbara, CA) and oxide-sharpened microfabricated Si_3N_4 cantilevers with a nominal spring constant of ~0.01 N/m (Microlevers, Veeco Metrology Group). The spring constants of the cantilevers were measured using the thermal noise method (Picoforce, Veeco Metrology Group).

Yeast cells were immobilized by mechanical trapping into porous polycarbonate membranes (Millipore, Billerica, MA) with a pore size similar to the cell size.[40] After filtering a cell culture, the filter was gently rinsed with the buffer, carefully cut (1 cm × 1 cm), attached to a steel sample puck using a small piece of double face adhesive tape, and the mounted sample was transferred into the AFM liquid cell while avoiding dewetting. Germinating cells were immobilized through hydrophobic attachment on solid substrata. To this end, glass coverslips coated with a thin layer of gold were immersed overnight in a 1 mM solution of 1-dodecanethiol (Sigma), rinsed with ethanol, and dried under N_2. After induction of germ tube formation in RPMI, the cells were harvested and rinsed three times in acetate buffer. Drops (200 μL) of the concentrated suspension were deposited on the hydrophobic substrates and left to stand for 3 h. After rinsing of the unattached cells with buffer, the substrates were analyzed by AFM. For single-molecule imaging, a cell was first localized using a bare tip, after which the tip was changed with an antibody or lectin-functionalized tip (see below). Adhesion maps were obtained by recording 32 × 32 force−distance curves on areas of given size, calculating the adhesion force for each force curve and displaying the value as a color pixel. Serum blocking experiments were performed by resuspending the cells in 15 μL/mL normal goat serum (Sigma) for 15 min at room temperature and washing them twice in buffer. For antibody and mannoside blocking experiments, buffer solutions containing free anti-Als3 antibodies (0.1 mg/mL) and methyl α-D-mannopyranoside (200 mM; Sigma) were injected into the AFM chamber. Unless specified otherwise, all force curves were recorded with a maximum applied force of 250 pN, using a constant approach and retraction speed of 1000 nm s^{-1}.

For single-molecule imaging, AFM tips were functionalized with anti-Als3 antibodies (kindly provided by Dr. Scott Filler, Harbor-UCLA Medical Center)[35] or with the Concavalin A lectin (ConA, Sigma) using ~6 nm long PEG−benzaldehyde linkers as described by Ebner *et al.*[25] Cantilevers were washed with chloroform and ethanol, placed in an UV-ozone cleaner for 30 min, immersed overnight into an ethanolamine solution (3.3 g of ethanolamine into 6 mL of DMSO), then washed three times with DMSO and two times with ethanol, and dried with N_2. The ethanolamine-coated cantilevers were immersed for 2 h in a solution prepared by mixing 1 mg of acetal-PEG-NHS dissolved in 0.5 mL of chloroform with 10 μL f triethylamine, then washed with chloroform, and dried with N_2. Cantilevers were further immersed for 5 min in a 1% citric acid solution, washed in Milli-Q water, and then covered with a 200 μL droplet of a PBS solution containing antibodies or lectins (0.2 mg/mL) to which 2 μL of a 1 M $NaCNBH_3$ solution was added. After 50 min, cantilevers were incubated with 5 μL of a 1 M ethanolamine solution in order to passivate unreacted aldehyde groups and then washed with and stored in buffer.

For quantifying cell surface hydrophobicity by means of chemical force microscopy,[31] hydrophobic tips were prepared by immersing gold-coated cantilevers (OMCL-TR4, Olympus Ltd., Tokyo, Japan; nominal spring constant ~0.02 N/m) for 12 h in 1 mM solutions of $HS(CH_2)_{11}CH_3$ in ethanol and then rinsed with ethanol. Force curves were recorded with a maximum applied force of 500 pN.

Conflict of Interest: The authors declare no competing financial interest.

Acknowledgment. Work at the Université catholique de Louvain was supported by the National Foundation for Scientific Research (FNRS), the Université catholique de Louvain (Fonds Spéciaux de Recherche), the Région Wallonne, the Federal Office for Scientific, Technical and Cultural Affairs (Interuniversity Poles of Attraction Programme), and the Research Department of the Communauté française de Belgique (Concerted Research Action). Work at Brooklyn College was supported by NIH Grants SC1 GM083756 and R01 GM098616. Work at VIB, KU Leuven was supported by Grant G.0804.11 from the Fund for Scientific Research Flanders. Y.F.D. and D.A. are Senior Research Associate and Postdoctoral Researcher of the FRS-FNRS. S.K. holds a postdoctoral fellowship of K.U. Leuven.

Supporting Information Available: Additional figures. This material is available free of charge *via* the Internet at http://pubs.acs.org.

REFERENCES AND NOTES

1. Costerton, J. W.; Stewart, P. S.; Greenberg, E. P. Bacterial Biofilms: A Common Cause of Persistent Infections. *Science* **1999**, *284*, 1318–1322.
2. Douglas, L. J. *Candida* Biofilms and Their Role in Infection. *Trends Microbiol.* **2003**, *11*, 30–36.
3. Finkel, J. S.; Mitchell, A. P. Genetic Control of *Candida albicans* Biofilm Development. *Nat. Rev. Microbiol.* **2011**, *9*, 109–118.
4. Kolter, R.; Greenberg, E. P. Microbial Sciences: The Superficial Life of Microbes. *Nature* **2006**, *441*, 300–302.
5. Dranginis, A. M.; Rauceo, J. M.; Coronado, J. E.; Lipke, P. N. A Biochemical Guide to Yeast Adhesins: Glycoproteins for Social and Antisocial Occasions. *Microbiol. Mol. Biol.* **2007**, *71*, 282–294.
6. Verstrepen, K. J.; Klis, F. M. Flocculation, Adhesion and Biofilm Formation in Yeasts. *Mol. Microbiol.* **2006**, *60*, 5–15.
7. Gow, N. A. R.; van de Veerdonk, F. L.; Brown, A. J. P.; Netea, M. G. *Candida albicans* Morphogenesis and Host Defence: Discriminating Invasion from Colonization. *Nat. Rev. Microbiol.* **2012**, *10*, 112–122.
8. Müller, D. J.; Dufrêne, Y. F. Atomic Force Microscopy: A Nanoscopic Window on the Cell Surface. *Trends Cell Biol.* **2011**, *21*, 461–469.
9. Müller, D. J.; Dufrêne, Y. F. Force Nanoscopy of Living Cells. *Curr. Biol.* **2011**, *21*, R212–R216.
10. Müller, D. J.; Dufrêne, Y. F. Atomic Force Microscopy as a Multifunctional Molecular Toolbox in Nanobiotechnology. *Nat. Nanotechnol.* **2008**, *3*, 261–269.
11. Müller, D. J.; Helenius, J.; Alsteens, D.; Dufrêne, Y. F. Force Probing Surfaces of Living Cells to Molecular Resolution. *Nat. Chem. Biol.* **2009**, *5*, 383–390.
12. Gad, M.; Itoh, A.; Ikai, A. Mapping Cell Wall Polysaccharides of Living Microbial Cells Using Atomic Force Microscopy. *Cell Biol. Int.* **1997**, *21*, 697–706.
13. Touhami, A.; Hoffmann, B.; Vasella, A.; Denis, F. A.; Dufrêne, Y. F. Aggregation of Yeast Cells: Direct Measurement of Discrete Lectin−Carbohydrate Interactions. *Microbiology* **2003**, *149*, 2873–2878.
14. Alsteens, D.; Garcia, M. C.; Lipke, P. N.; Dufrêne, Y. F. Force-Induced Formation and Propagation of Adhesion Nanodomains in Living Fungal Cells. *Proc. Natl. Acad. Sci. U.S.A.* **2010**, *107*, 20744–20749.
15. Alsteens, D.; Dupres, V.; Mc Evoy, K.; Wildling, L.; Gruber, H. J.; Dufrêne, Y. F. Structure, Cell Wall Elasticity and Polysaccharide Properties of Living Yeast Cells, as Probed by AFM. *Nanotechnology* **2008**, *19*, 384005.
16. Dupres, V.; Alsteens, D.; Wilk, S.; Hansen, B.; Heinisch, J. J.; Dufrêne, Y. F. The Yeast Wsc1 Cell Surface Sensor Behaves Like a Nanospring *in Vivo*. *Nat. Chem. Biol.* **2009**, *5*, 857–862.
17. Heinisch, J. J.; Dupres, V.; Wilk, S.; Jendretzki, A.; Dufrêne, Y. F. Single-Molecule Atomic Force Microscopy Reveals Clustering of the Yeast Plasma-Membrane Sensor Wsc1. *PloS One* **2010**, *5*, e11104.
18. Kucharíková, S.; Tournu, H.; Lagrou, K.; van Dijck, P.; Bujdáková, H. Detailed Comparison of *Candida albicans* and *Candida glabrata* Biofilms under Different Conditions and Their Susceptibility to Caspofungin and Anidulafungin. *J. Med. Microbiol.* **2011**, *60*, 1261–1269.
19. Hazen, B. W.; Hazen, K. C. Dynamic Expression of Cell Surface Hydrophobicity during Initial Yeast Cell Growth and before Germ Tube Formation of *Candida albicans*. *Infect. Immun.* **1988**, *56*, 2521–2525.
20. Hoyer, L. L. The ALS Gene Family of *Candida albicans*. *Trends Microbiol.* **2001**, *9*, 176–180.
21. Liu, Y.; Filler, S. G. *Candida albicans* Als3, a Multifunctional Adhesin and Invasin. *Eukaryotic Cell* **2011**, *10*, 168–173.
22. Nobile, C. J.; Andes, D. R.; Nett, J. E.; Smith, F. J., Jr.; Yue, F.; Phan, Q. T.; Edwards, J. E.; Filler, S. G.; Mitchell, A. P. Critical Role of Bcr1-Dependent Adhesins in *C. albicans* Biofilm Formation *in Vitro* and *in Vivo*. *PLoS Pathog.* **2006**, *2*, 636–649.
23. Nobile, C. J.; Schneider, H. A.; Nett, J. E.; Sheppard, D. C.; Filler, S. G.; Andes, D. R.; Mitchell, A. P. Complementary Adhesin Function in *C. albicans* Biofilm Formation. *Curr. Biol.* **2008**, *18*, 1017–1024.
24. Coleman, D. A.; Oh, S. H.; Zhao, X.; Zhao, H.; Hutchins, J. T.; Vernachio, J. H.; Patti, J. M.; Hoyer, L. L. Monoclonal Antibodies Specific for *Candida albicans* Als3 That Immunolabel Fungal Cells *in Vitro* and *in Vivo* and Block Adhesion to Host Surfaces. *J. Microbiol. Methods* **2009**, *78*, 71–78.
25. Ebner, A.; Wildling, L.; Kamruzzahan, A. S. M.; Rankl, C.; Wruss, J.; Hahn, C. D.; Hölzl, M.; Zhu, R.; Kienberger, F.; Blass, D.; *et al.* A New, Simple Method for Linking of Antibodies to Atomic Force Microscopy Tips. *Bioconjugate Chem.* **2007**, *18*, 1176–1184.
26. Alsteens, D.; Dupres, V.; Klotz, S. A.; Gaur, N. K.; Lipke, P. N.; Dufrêne, Y. F. Unfolding Individual Als5p Adhesion Proteins on Live Cells. *ACS Nano* **2009**, *3*, 1677–1682.
27. Yoshijima, Y.; Murakami, K.; Kayama, S.; Liu, D.; Hirota, K.; Ichikawa, T.; Miyake, Y. Effect of Substrate Surface Hydrophobicity on the Adherence of Yeast and Hyphal *Candida*. *Mycoses* **2010**, *53*, 221–226.
28. Masuoka, J.; Hazen, K. C. Cell Wall Protein Mannosylation Determines *Candida albicans* Cell Surface Hydrophobicity. *Microbiology* **1997**, *143*, 3015–3021.
29. Ener, B.; Douglas, L. J. Correlation between Cell-Surface Hydrophobicity of *Candida albicans* and Adhesion to Buccal Epithelial Cells. *FEMS Microbiol. Lett.* **1992**, *99*, 37–42.
30. Fu, Y.; Ibrahim, A. S.; Sheppard, D. C.; Chen, Y. C.; French, S. W.; Cutler, J. E.; Filler, S. G.; Edwards, J. E., Jr. *Candida albicans* Als1p: An Adhesin That Is a Downstream Effector of the EFG1 Filamentation Pathway. *Mol. Microbiol.* **2002**, *44*, 61–72.
31. Dague, E.; Alsteens, D.; Latgé, J. P.; Verbelen, C.; Raze, D.; Baulard, A. R.; Dufrêne, Y. F. Chemical Force Microscopy of Single Live Cells. *Nano Lett.* **2007**, *7*, 3026–3030.
32. Cheng, S. C.; van de Veerdonk, F. L.; Lenardon, M.; Stoffels, M.; Plantinga, T.; Smeekens, S.; Rizzetto, L.; Mukaremera, L.; Preechasuth, K.; Cavalieri, D.; *et al.* The Dectin-1/Inflammasome Pathway Is Responsible for the Induction of Protective T-Helper 17 Responses That Discriminate between Yeasts and Hyphae of *Candida albicans*. *J. Leukocyte Biol.* **2011**, *90*, 357–366.
33. Lipke, P. N.; Garcia, M. C.; Alsteens, D.; Ramsook, C. B.; Klotz, S. A.; Dufrêne, Y. F. Strengthening Relationships: Amyloids Create Adhesion Nanodomains in Yeasts. *Trends Microbiol.* **2012**, *20*, 59–65.
34. Hazen, K. C.; Hazen, B. W. A Polystyrene Microsphere Assay for Detecting Surface Hydrophobicity Variations within *Candida albicans* Populations. *J. Microbiol. Methods* **1987**, *6*, 289–299.
35. Phan, Q. T.; Myers, C. L.; Fu, Y.; Sheppard, D. C.; Yeaman, M. R.; Welch, W. H.; Ibrahim, A. S.; Edwards, J. E., Jr.; Filler, S. G. Als3 Is a *Candida albicans* Invasin That Binds to

Cadherins and Induces Endocytosis by Host Cells. *PLoS Biol.* **2007**, *5*, 0543–0557.
36. Vogel, V.; Sheetz, M. Local Force and Geometry Sensing Regulate Cell Functions. *Nat. Rev. Mol. Cell. Biol.* **2006**, *7*, 265–275.
37. Gillum, A. M.; Tsay, E. Y. H.; Kirsch, D. R. Isolation of the *Candida albicans* Gene for Orotidine-5′-Phosphate Decarboxylase by Complementation of *S. cerevisiae ura3* and *E. coli pyrF* Mutations. *Mol. Genet. Genomics* **1984**, *198*, 179–182.
38. Fonzi, W. A.; Irwin, M. Y. Isogenic Strain Construction and Gene Mapping in *Candida albicans*. *Genetics* **1993**, *134*, 717–728.
39. Mora-Montes, H. M.; Bates, S.; Netea, M. G.; Castillo, L.; Brand, A.; Buurman, E. T.; Diaz-Jimenez, D. F.; Jan Kullberg, B.; Brown, A. J.; Odds, F. C.; *et al.* A Multifunctional Mannosyltransferase Family in *Candida albicans* Determines Cell Wall Mannan Structure and Host-Fungus Interactions. *J. Biol. Chem.* **2010**, *285*, 12087–12095.
40. Dufrêne, Y. F. Atomic Force Microscopy and Chemical Force Microscopy of Microbial Cells. *Nat. Protoc.* **2008**, *3*, 1132–1138.